

Tourmaline from the rare-element Pinilla pegmatite, (Central Iberian Zone, Zamora, Spain): chemical variation and implications for pegmatitic evolution

E. Roda-Robles¹, A. Pesquera¹, P. P. Gil¹, J. Torres-Ruiz²,
and F. Fontan³

¹Departamento de Mineralogía y Petrología, Facultad de Ciencia y Tecnología, Universidad País Vasco (UPV/EHU), Bilbao, Spain

²Departamento de Mineralogía y Petrología, Facultad de Ciencias, Universidad Granada, Spain

³Laboratoire Cristallographie et Minéralogie, URA-067-Université Paul Sabatier Toulouse, France

Received September 21, 2003; accepted January 23, 2004

Editorial handling: A. Beran and E. Libowitzky

Summary

Tourmaline is an ubiquitous constituent in the Pinilla de Fermoselle rare-element pegmatite (Zamora, Spain), as well as in barren pegmatitic and quartz–tourmaline veins inside the associated leucogranite. The rare-element pegmatite shows internal zoning, evolving from a barren facies, in the lower border zone, in contact with the leucogranite, to a Li-rich facies in the upper border zone, close to the host-rocks.

Tourmalines from the veins within the leucogranite have highest Mg contents, and belong to the schorl–dravite series. The tourmalines from the rare-element pegmatite mostly belong to the schorl–elbaite series, with chemical compositions within the range of the end-members, whereas the tourmalines associated with the most evolved zone in the pegmatite belong to the elbaite–rossmanite series. The broad compositional range shown by the tourmalines correlates quite well with the pegmatite zoning. The most plausible substitution mechanism for the chemical evolution of tourmalines during crystallization seems to be $\text{Mg}_{-1}\text{Fe}^{2+}_1, [\text{X}]_{-1}^{\text{Y}}\text{Al}_{-1}\text{XNa}_1^{\text{Y}}\text{Fe}^{2+}_1$, for the foitite–schorl series; $^{\text{Y}}\text{Fe}^{2+}_{-3}{}^{\text{Y}}\text{Al}_{1.5}{}^{\text{Y}}\text{Li}_{1.5}$, for the schorl–elbaite vector; $^{\text{X}}\text{Na}_{-1}{}^{\text{Y}}\text{Li}_{-0.5}[\text{X}]_1^{\text{Y}}\text{Al}_{0.5}$, for the elbaite–rossmanite series; and, $(\text{OH})_1\text{F}_1$ for all the tourmalines except the pink elbaites. This chemical variation in tourmaline is consistent with a crystal fractionation model for the evolution of the Pinilla pegmatite.

Introduction

The Pinilla de Fermoselle area (Zamora, Spain) is located in the northwestern limit of the Tormes Dome, which belongs to the Central Iberian Zone (Fig. 1). The Pinilla pegmatite is associated with a peraluminous leucogranite, included in the group of syntectonic massifs, which have been affected by the third phase of Hercynian deformation (*López Plaza and Carnicero, 1988*).

The granitic outcrops are separated by narrow belts of Precambrian and Cambrian metamorphic rocks of the schist-metagreywacke complex (CEG), comprising a sequence of micaceous schists and carbonates with layers of quartzite. These have undergone Hercynian deformation and metamorphism (*Martínez Fernandez, 1974*).

The Li-bearing pegmatite is located between the Pinilla de Fermoselle leucogranite and the metamorphic country-rocks (Figs. 1 and 2). A complete evolutionary sequence is observed in the pegmatitic body, from the contact with leucogranite in its footwall, to the contact with hornfels in its hangingwall. Based on parageneses, textural characteristics and chemical composition, three distinct zones with an asymmetric distribution are distinguished in the pegmatitic body (Fig. 2). Tourmaline is present in these three zones, and it is also a common constituent in barren pegmatitic and quartz–tourmaline veins inside the associated leucogranite.

This study deals principally with the chemical variation of tourmaline in the pegmatites and hydrothermal veins, and its implications for the evolution of this pegmatite.

Geology of the pegmatitic body

The three zones distinguished in the pegmatitic body are sub-horizontally disposed, exhibiting different degrees of differentiation, which increases from the footwall contact with the leucogranite towards the hangingwall contact with the hornfels. From the base of the Pinilla pegmatite upward to the top, the following sequence is developed (Fig. 2):

- (1) Lower border zone (≈ 3 m thick): It is in contact with the leucogranite. It mainly consists of K-feldspar, quartz, muscovite, albite and biotite, with minor tourmaline. Graphic intergrowths of quartz and K-feldspar are common. A gradual increase in grain size from the granitic (up to 2 mm) to the pegmatitic facies (up to 7 cm) may be observed in places.
- (2) Intermediate zone (2–6 m thick), just above the lower border zone (1), and where blocky quartz is located. It is characterized by the occurrence of nodules of Fe–Mn phosphates (up to ≈ 65 cm long). The most abundant phosphates are ferrisicklerite, heterosite and alluaudite, showing Fe/(Fe + Mn) ratios from 0.64 to 0.67 (for more information about these phosphates see *Roda et al., 1998*). The other main minerals are quartz and muscovite. K-feldspar, albite, tourmaline and zinnwaldite are also common in this zone.

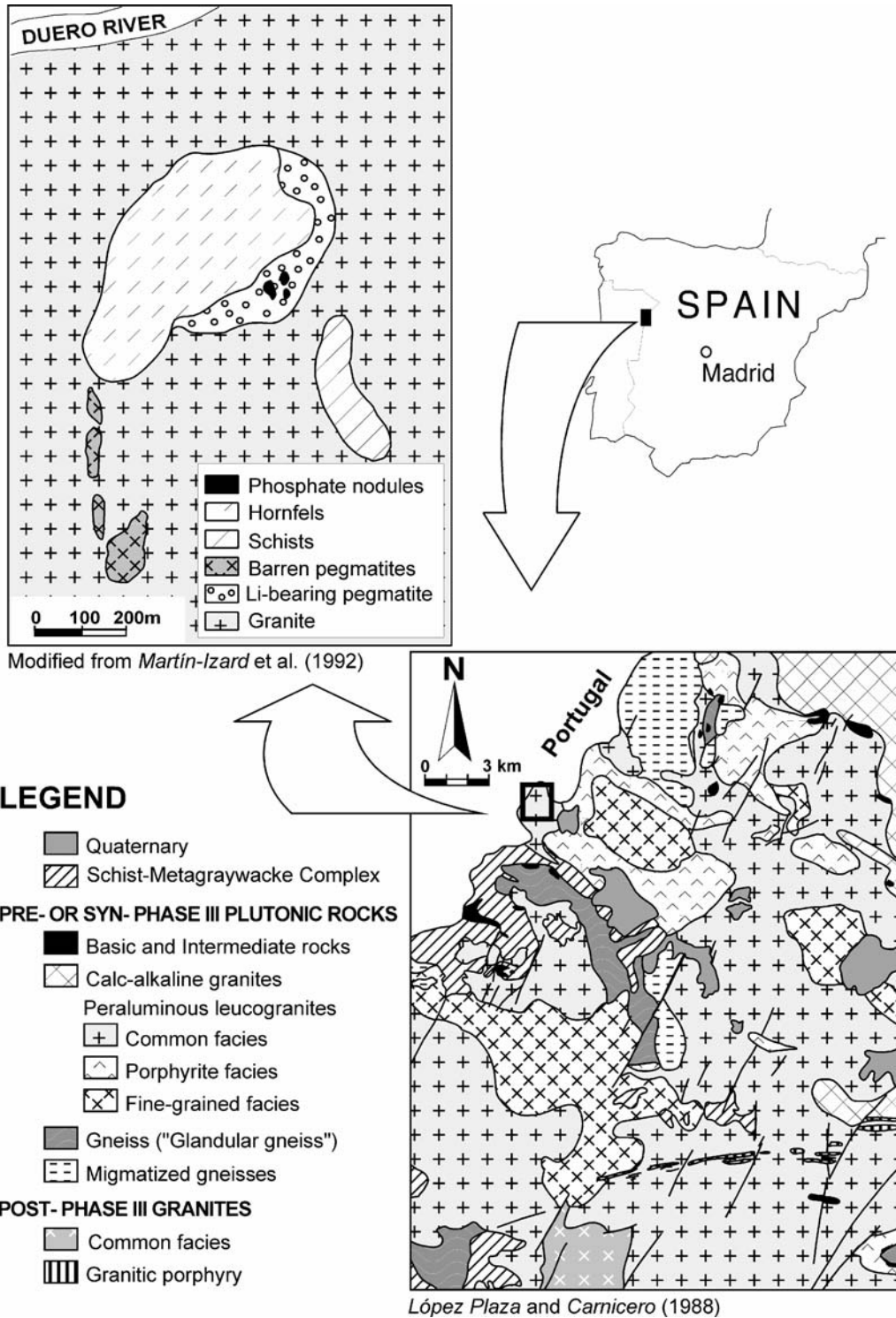


Fig. 1. Schematic geological map of the Pinilla de Femoselle area (Zamora, Spain)

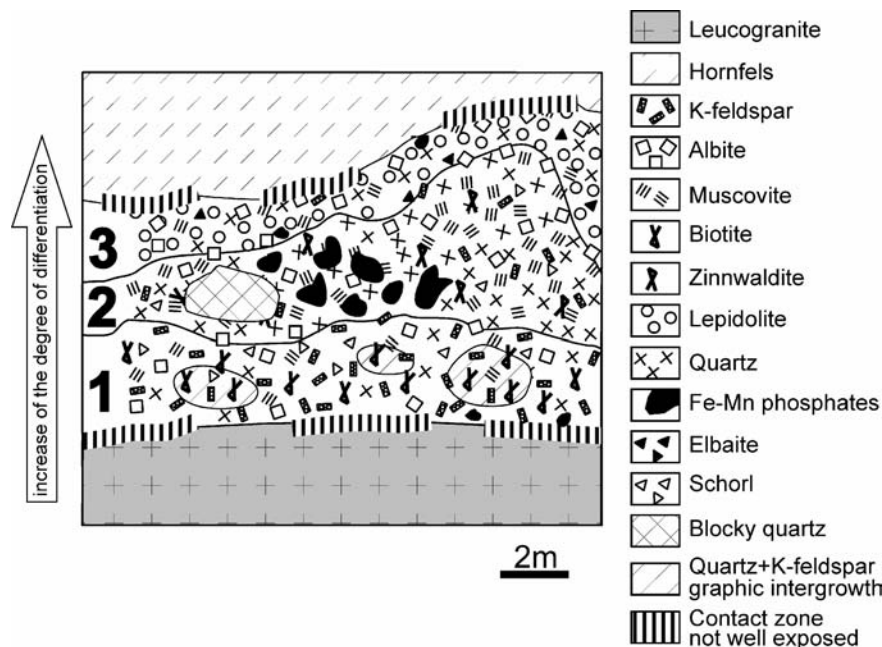


Fig. 2. Idealized section of the Pinilla de Feroselle pegmatite. Showing zones 1 to 3

- (3) Upper border zone, close to the hornfels. It is the narrowest zone of the body, commonly less than 2 m thick. Quartz, micas of the muscovite–lepidolite series, albite and K-feldspar are the main minerals, with Li–tourmaline as minor constituent. As accessory minerals Fe–Mn phosphates, apatite, cassiterite, beryl, and zircon appear.

In addition to the three zones of the pegmatite, tourmaline is also associated with barren pegmatitic and quartz–tourmaline veins within the leucogranite. Both, barren pegmatites and quartz–tourmaline veins are rare and occur exclusively near the contact with the rare-element pegmatite, but never inside it. Quartz–tourmaline veins appear as thin elongated lenses (<10 cm thick), with up to ≈ 1 m length. The pegmatitic segregations inside the leucogranite consist of quartz + K-feldspar \pm tourmaline \pm muscovite. A preferential orientation has not been observed for these tourmaline-bearing veins within the leucogranite.

No pervasive tourmalinization has been observed in the country rocks, and thus, tourmaline is not present in the hornfels above the pegmatitic body.

Sampling and analytical methods

The mineral samples studied have been selected from the three zones of the pegmatite body, as well as from the veins inside the associated leucogranite. Some of the samples were prepared by hand picking, and later examined with a binocular microscope and ground in an automatic agate pulverizer.

Major element analyses were performed on polished thin sections with a Cameca SX50 electron microprobe, equipped with four wavelength-dispersive

spectrometers at the University of Granada. The operating conditions were: accelerating voltage of 20 kV, with a beam current of 30 nA, and a beam diameter of about 1 μm . Both natural and synthetic standards were used: natural fluorite (F), natural sanidine (K), natural pollucite (Cs), synthetic MnTiO_3 (Ti, Mn), natural diopside (Ca), synthetic BaSO_4 (Ba), synthetic Fe_2O_3 (Fe), natural albite (Na), natural periclase (Mg), synthetic SiO_2 (Si), natural apatite (P), and synthetic Al_2O_3 (Al).

Trace elements, including Rb, Be, Sr, Ba, Sc, V, Cr, Co, Ni, Cu, Zn, Ga, Y, Nb, Ta, Zr, Hf, Mo, Sn, Tl, Pb, U, Th, W, and REE were analyzed at the University of Granada using an inductively coupled plasma mass spectrometry (ICP-MS) technique with Perkin Elmer SCIEX Elan-5000 equipment. Li contents were determined for some samples using atomic absorption spectrometry (AAS).

Some representative samples were also analyzed with an X-ray diffractometer using Si as internal standard, by scanning through $5\text{--}70^\circ 2\theta$ using $\text{CuK}\alpha$ radiation (Step size = $0.02^\circ 2\theta$ and time per step = 1 s.). Unit cell dimensions were obtained using the FullProf software (*Rodríguez-Carvajal, 1998*).

Textural characteristics of tourmaline

Tourmaline shows important petrographic and compositional changes from the veins inside the leucogranite to the barren zone 1, and from this barren zone to the most evolved zone 3.

In the barren pegmatitic and quartz–tourmaline veins within the leucogranite, tourmaline is always associated with quartz. These veins frequently exhibit a symmetric zoning. In the quartz–tourmaline veins, the general type of zoning is expressed by quartz in the core zone and in tourmaline in the border zone; however the opposite zoning was also observed. In the pegmatitic segregations, quartz appears in the core zone, tourmaline in the intermediate zone; the border zone consists of quartz + K-feldspar \pm muscovite. In both cases, tourmaline forms black, fine-to medium-grained sub- to euhedral crystals. Under the microscope this tourmaline commonly exhibits a chromatic zonation, mainly in the euhedral crystals, with a core zone showing strong pleochroism from deep brown to olive green, whereas the border zone changes from reddish brown to reddish orange.

Inside the rare-element pegmatite, tourmaline in zone 1 is black and appears as prismatic–columnar, fine-to medium-grained crystals. Under the microscope it is slightly pleochroic, commonly with brownish orange and olive green tones.

Tourmaline from zone 2 mainly appears as black, subhedral medium grained crystals, and under the microscope it exhibits slight pleochroism from orange to light green. Rarely there are small-scale lobate intergrowths with plagioclase, similar to those described by *Gaweda et al. (2002)* for tourmalines associated with barren pegmatites. Besides the black tourmaline, dark-green tourmalines are also observed in zone 2, near the Fe–Mn phosphate masses, but never in direct contact with the phosphates. It is fine to medium grained and shows concentric chromatic zoning with intense pleochroism, ranging from brownish orange to light green in the core and from deep brown to reddish brown in the border zone of the crystals. In this zone tourmaline crystals frequently reveal the effects of deformation, such as undulant extinction, development of subgrains and deformation bands.

In the most evolved zone 3 both green and pink medium sized prismatic crystals of elbaite are common. Green elbaite is always associated with medium sized muscovite and quartz, whereas pink elbaite appears in association with fine-grained lepidolite, albite and quartz. Under the microscope elbaite grains are colourless or slightly coloured (light bluish grey).

Results

Chemical composition

Most of the tourmalines analysed belong to the schorl–elbaite series, with chemical compositions ranging between the two end-members (Table 1, Fig. 3). Some of the tourmalines associated with the barren veins within the leucogranite are richer in Mg, and belong to the schorl–dravite series, always closer to the Fe-rich end-member. These chemical data are consistent with the X-ray diffraction data, with the *a* and *c* parameters of most of the tourmalines plotting close to the elbaite–schorl reference line (JCPDF reference data: schorl = 43–1464, elbaite = 49–1833 and dravite = 81–1535; rossmanite data from *Selway et al.*, 1998) (Fig. 4).

Cations per formula unit were calculated on the basis of the structural formula $XY_3Z_6(BO_3)_3T_6O_{18}V_3W$, for which X = Na, Ca, K, vacancy; Y = Mg, Fe²⁺, Fe³⁺, Li⁺, Al, Mn, Ti⁴⁺, Cr³⁺; Z = Al, Mg, Fe²⁺, Fe³⁺, Cr³⁺; T = Si, Al; V = OH⁻, O²⁻, W = OH⁻, O²⁻, F⁻, Cl⁻. The Li contents were estimated following the procedure used by previous investigators, (e.g. *Morgan and London*, 1987; and *Burns et al.*, 1994), assuming both boron and OH + F as stoichiometric (B = 3 and OH + F = 4 atoms per formula unit (apfu) respectively). The amount of Li assigned to the Y-site is the ideal sum of the Y-site cations (3 apfu) minus the sum of the other cations occupying this site. Analyses have been normalized to 24.5 oxygens. Some tourmaline samples from the three zones of the pegmatite were analyzed for Li by atomic absorption. These data correlate quite well with the results of stoichiometric calculations, although systematically these latter Li₂O values are ≈0.2 wt% higher than those obtained by atomic absorption. For the calculations all the Mn and Fe were assumed to be divalent, although a certain proportion of Fe³⁺ may be present in both Y-site and Z-site. Mössbauer data would be necessary to establish the presence of oxidized iron in the tourmalines studied.

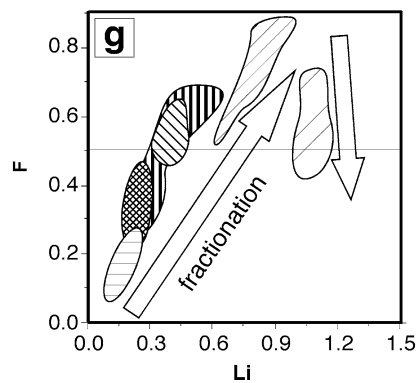
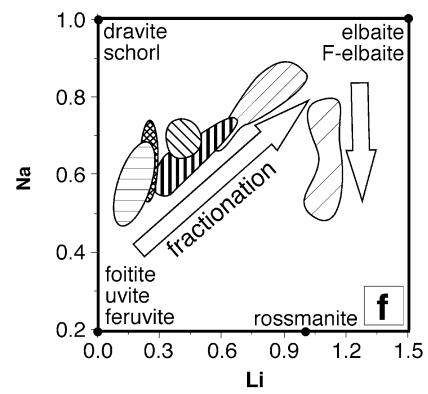
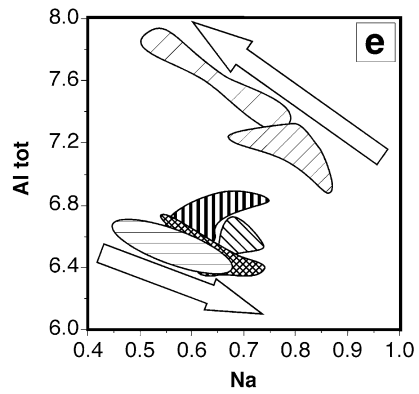
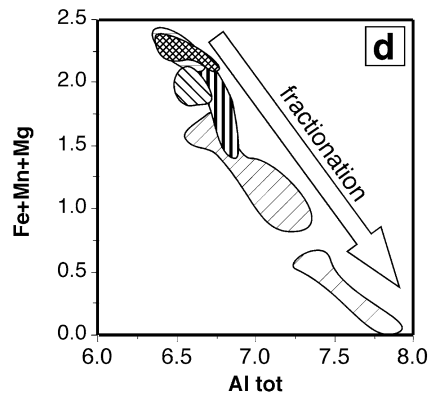
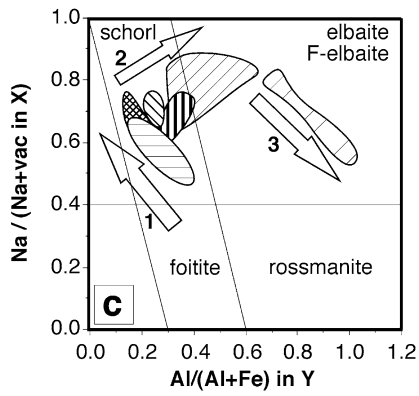
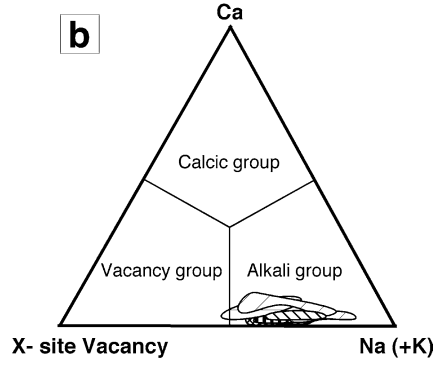
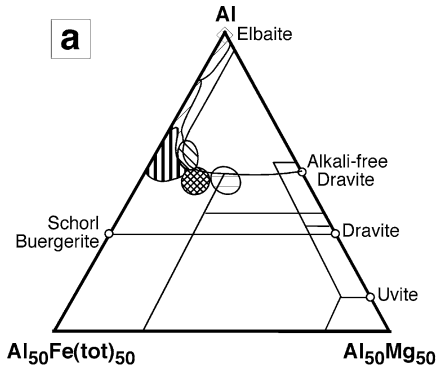
Overall, important variations occur for Al₂O₃ (32.81–42.70 wt%), FeO (0.00–15.00 wt%), MgO (0.00–5.25 wt%), Li₂O (0.169–1.76 wt%), MnO (0.05–1.09 wt%), Na₂O (1.56–2.72 wt%), F (0.16–1.69 wt%), and TiO₂ (0.00–1.19 wt%). Smaller variations are observed for CaO (0.00–0.45 wt%) and ZnO (0.00–0.33 wt%). The highest Zn contents for tourmaline are observed in some green schorls from zone 2 (Table 1). The contents in K₂O (0.00–0.06 wt%), Cr₂O₃ (0.00–0.03 wt%), and Cl (0.00–0.03 wt%) are negligible. Fe (defined as Fe_{total}/(Fe_{total} + Mg)) varies from 0.81 to 1.00 in the tourmalines from the pegmatite, and from 0.47 to 0.73 for the pegmatitic and the quartz–tourmaline veins within the leucogranite. Representation of the chemical data on the Al–Fe–Mg diagram (*Henry and Guidotti*, 1985) (Fig. 3a) shows a broad compositional range that correlates quite well with the tourmaline-bearing zone of the pegmatite. Thus, tourmalines associated with the pegmatitic and the quartz–tourmaline veins

Table 1. *Representative microprobe analyses (wt.%) of tourmalines*

Zone	Veins inside granite		1		2		3			
	black		black		black	dark green	green	pink		
SiO ₂	36.57	35.74	35.33	35.44	35.12	35.85	35.91	36.47	38.34	38.74
TiO ₂	0.39	1.19	0.46	0.92	0.47	0.05	0.02	0.00	0.00	0.00
Al ₂ O ₃	34.54	33.58	33.53	33.27	33.18	35.34	37.29	38.14	42.42	41.99
FeO/tot	8.60	8.57	10.38	11.08	11.65	11.25	8.42	5.92	0.10	0.02
MnO	0.06	0.07	0.11	0.09	0.16	0.24	0.33	0.81	0.54	0.61
MgO	4.33	4.84	3.21	2.80	1.41	0.14	0.01	0.01	0.00	0.00
ZnO	0.04	0.06	0.11	0.12	0.22	0.30	0.28	0.17	0.14	0.04
CaO	0.13	0.38	0.08	0.06	0.03	0.03	0.06	0.13	0.30	0.40
Na ₂ O	1.60	1.98	1.96	2.01	2.16	2.10	2.17	2.52	1.68	1.80
K ₂ O	0.03	0.05	0.04	0.05	0.04	0.03	0.03	0.03	0.02	0.02
F	0.25	0.39	0.59	0.71	1.00	1.20	1.02	1.30	0.87	1.11
O = F	0.11	0.17	0.25	0.30	0.42	0.51	0.43	0.55	0.37	0.47
H ₂ O*	3.57	3.49	3.33	3.28	3.08	3.06	3.17	3.07	3.40	3.30
B ₂ O ₃ *	10.69	10.65	10.45	10.49	10.33	10.52	10.58	10.70	11.05	11.09
LiO ₂ *	0.23	0.30	0.33	0.40	0.61	0.81	0.98	1.28	1.58	1.76
Total	100.93	101.16	99.66	100.43	99.05	100.42	99.83	100.01	100.10	100.42
B	3.000	3.000	3.000	3.000	3.000	3.000	3.000	3.000	3.000	3.000
Si	5.948	5.832	5.879	5.872	5.913	5.922	5.899	5.925	6.033	6.075
Al(IV)	0.052	0.168	0.121	0.128	0.087	0.078	0.101	0.075	0.000	0.000
Al(Z)	6.000	6.000	6.000	6.000	6.000	6.000	6.000	6.000	6.000	6.000
Al(Y)	0.571	0.291	0.457	0.370	0.499	0.805	1.122	1.228	1.869	1.762
Ti	0.047	0.146	0.058	0.115	0.060	0.007	0.002	0.001	0.000	0.000
Fe ²⁺	1.170	1.170	1.444	1.536	1.640	1.554	1.157	0.804	0.013	0.003
Mn	0.009	0.010	0.015	0.013	0.023	0.034	0.046	0.112	0.072	0.082
Mg	1.049	1.177	0.796	0.692	0.355	0.035	0.003	0.002	0.000	0.000
Zn	0.005	0.008	0.014	0.014	0.028	0.037	0.034	0.021	0.016	0.005
Y total	2.851	2.802	2.784	2.740	2.605	2.471	2.364	2.167	1.971	1.852
Li*	0.149	0.198	0.216	0.260	0.395	0.529	0.636	0.833	1.029	1.148
Ca	0.022	0.067	0.015	0.010	0.005	0.005	0.010	0.022	0.051	0.067
Na	0.505	0.626	0.632	0.647	0.705	0.674	0.690	0.793	0.513	0.547
K	0.006	0.010	0.008	0.010	0.008	0.006	0.007	0.006	0.004	0.004
X total	0.533	0.702	0.655	0.667	0.718	0.685	0.707	0.821	0.568	0.617
F	0.128	0.203	0.308	0.371	0.535	0.627	0.528	0.669	0.434	0.550
OH*	3.871	3.797	3.692	3.629	3.465	3.373	3.472	3.331	3.566	3.450
Fe/(Fe + Mg)	0.53	0.50	0.64	0.69	0.82	0.98	1.00	1.00	1.00	1.00
Na/(Na + Ca)	0.96	0.90	0.98	0.98	0.99	0.99	0.99	0.97	0.91	0.89

* calculated (see text)

within the leucogranite carry the highest, but variable, Mg contents. Following the nomenclature proposed by *Selway and Novák (1997)*, they are classified as schorl–dravite (Mg occupies 45.12% of Y-site), to Mg-rich schorl (30.48% of the Y-site occupied by Mg). The rest of the analysed tourmalines, i.e. those associated with the rare-element pegmatite, show low contents of Mg and Ca, which indicates minor amounts of the dravite and uvite components. Tourmaline from the barren zone 1 of the pegmatitic body shows schorl-rich compositions. Tourmaline



- × pegmatitic vein inside leucogranite
- ○ 1 (black)
- ▨ □ 2 (black)
- ▨ △ 2 (dark green)
- + 3 (green)
- ◇ 3 (pink)

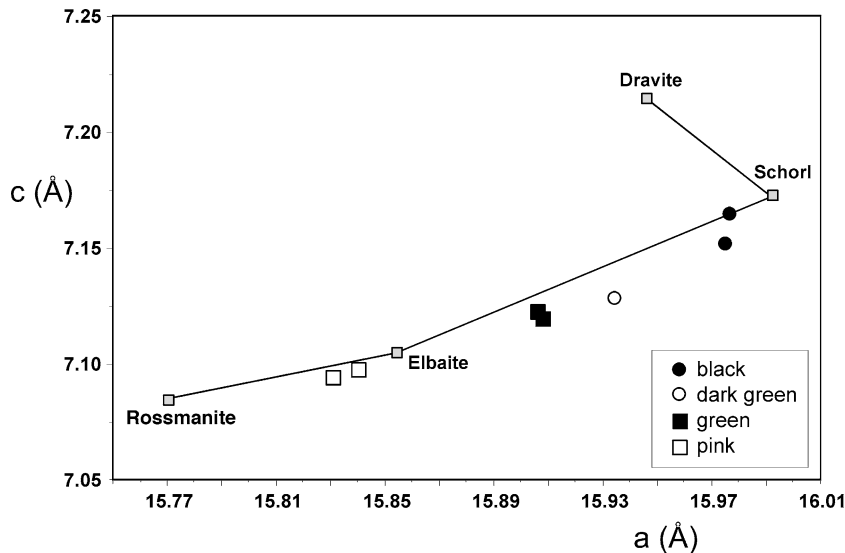


Fig. 4. Unit-cell dimensions of representative tourmaline samples

associated with the intermediate zone 2 is poorer in Mg and richer in Al than those tourmalines from zone 1. Green tourmaline from the evolved zone 3 shows higher Al-contents, and, finally, pink elbaite is the Al-richest tourmaline (Fig. 3a).

The tourmalines are classified as members of the alkali tourmaline group because of the predominance of Na at this site (*Hawthorne and Henry, 1999*) (Fig. 3b). The chemical composition of tourmaline evolved through the following sequence from the veins inside the leucogranite to the most evolved zone 3 in the pegmatite (Table 1, Fig. 3c): (1) tourmalines associated with the pegmatitic and the quartz–tourmaline veins inside the leucogranite change from schorl–dravite to Mg-rich schorl, with a high foitite component in all the cases; (2) in zone 1, inside the rare-element pegmatite, tourmaline compositions vary from Mg-rich schorl (with a high foitite component) to Al-rich schorl (with minor vacancies in the X-site); (3) in the intermediate zone 2 two different groups of tourmalines have been distinguished: (a) black tourmaline crystals associated with muscovite, quartz and K-feldspar, with a composition belonging to Al-rich schorl; and, (b) dark green tourmaline crystals appearing near the Fe–Mn phosphate masses, with a chemical composition ranging from Al-rich schorl to Li-rich schorl; (4) in the most evolved zone 3, tourmaline composition ranges from schorl–elbaite (green crystals) to elbaite with a high rossmanite component (pink crystals) (Fig. 3c).



Fig. 3. Plots of the chemical composition of tourmalines from the Pinilla de Feroselle pegmatite. **a** Al–Fe_{total}–Mg diagram (in molecular proportions; after *Henry and Guidotti, 1985*); **b** X-site ternary plot of Na + K–Ca–X-site vacancy; **c** variation in Na/(Na + Ca) at the X site versus Al/(Al + Fe) at the Y site; **d** variation of Al total versus Fe + Mn + Mg (apfu); **e** variation of Na versus Al total (apfu); **f** variation of Li versus Na (apfu); **g** variation of Li versus F (apfu)

Table 2. Representative ICP analyses of tourmalines (ppm)

Zone	1	2	3								
Color	black	dark green	green	pink							
Rb	11.7	155.9	148.4	16.6	7.8	9.9	38.5	27.2	12.4	3.3	
Cs	2.0	47.5	17.6	3.6	0.4	2.1	22.7	9.9	0.6	0.4	
Be	10.1	6.0	7.5	6.6	4.9	8.0	21.8	25.4	46.5	21.7	
Sr88	3.0	0.4	6.0	0.6	0.0	0.1	0.4	0.2	0.0	0.0	
Ba	1.4	0.8	2.4	1.1	0.0	0.5	1.0	0.6	0.0	0.0	
Ni	2.4	1.3	1.6	0.7	1.9	1.1	3.0	1.6	1.4	0.9	
Cu	4.3	1.9	8.6	1.8	4.1	1.8	2.1	3.4	1.0	0.6	
Ga	88.8	82.3	90.7	117.2	70.7	121.3	111.9	94.9	92.7	108.1	
Y	0.1	0.8	0.3	0.1	0.0	0.1	0.1	0.1	0.0	0.0	
Nb	1.7	22.9	2.0	1.8	1.5	3.7	6.0	8.9	6.2	6.9	
Ta	1.7	3.8	1.3	0.7	0.6	1.2	6.2	7.8	3.5	4.5	
Zr	2.2	45.1	1.9	2.9	1.0	2.0	2.3	1.6	0.8	0.9	
Hf	0.1	2.0	0.1	0.1	0.0	0.1	0.4	0.2	0.1	0.2	
Mo	0.0	0.1	0.1	0.1	0.1	0.1	0.1	0.1	0.1	0.1	
Sn	34.1	70.2	128.3	143.2	96.5	198.4	281.5	393.2	277.6	294.6	
W	0.4	3.1	0.6	0.3	0.6	0.4	0.3	0.4	0.2	0.1	
Tl	1.7	3.8	1.3	0.7	0.6	1.2	6.2	7.8	3.5	4.5	
Pb	2.2	2.6	11.2	12.4	1.9	4.7	13.1	15.5	2.7	8.1	
U	0.2	5.5	0.8	1.2	0.7	0.5	0.3	0.4	0.1	0.2	
Th	0.1	4.0	0.0	0.1	0.0	0.0	0.8	0.9	0.0	0.1	
ΣLREE	0.4	9.77	0.28	1.10	0.00	0.29	0.43	0.84	0.00	0.02	
ΣHREE	0.0	0.94	0.07	0.03	0.01	0.02	0.04	0.11	0.00	0.01	

The trace elements are very low, for all the analysed tourmalines, except for Rb, Cs, Be, Ga, Nb, Ta and Sn (Table 2). In general, REE-contents are very low, except for the dark green tourmalines from zone 2. This anomalous content in REE in comparison with the rest of the analysed tourmalines may be due to the contamination of the sample with zircon, which also would explain the higher contents in Zr, U, and Th shown by this sample (Table 2). Trace element concentrations in general do not change along the zones with the exception of Sn, (Nb and Ta) contents, which increased with increasing differentiation (Table 2).

Substitution schemes

The plot of $\text{Na}/(\text{Na} + \text{vacancies})$ vs. $\text{Al}/(\text{Al} + \text{Fe})$ reflects the two main substitutions developed in tourmalines: $\text{Na} \Leftrightarrow [\text{X}]$ and $\text{Al} \Leftrightarrow \text{Fe}$ (Fig. 3c). This diagram does not show the substitution $\text{Fe}^{2+}\text{Mg}_{-1}$, and for this reason, tourmalines with >1 apfu Mg, normally belonging to the schorl–dravite series, should not be plotted on it (Selway et al., 1999). As all the Mg-rich tourmalines are closer to the schorl end-member than to the dravite end-member, all our data have been plotted. Nevertheless, the clear negative correlation of Mg and Fe in tourmalines from the pegmatitic and quartz–tourmaline veins within the leucogranite and from zone 1 suggests that the FeMg_{-1} exchange vector must have been important in these

tourmalines (Table 1). The three different vectors (1 to 3) in Fig. 3c correspond to evolutionary series from foitite to schorl to elbaite to rossmanite, representing increasing fractionation. Such vectors represent three solid-solution series:

- (1) foitite–schorl: $[X] + {}^YAl \Leftrightarrow {}^XNa + {}^YFe^{2+}$;
- (2) schorl–elbaite: ${}^YFe^{2+}_3 \Leftrightarrow {}^YAl_{1.5} + {}^YLi_{1.5}$;
- (3) elbaite–rossmanite: ${}^XNa + {}^YLi_{0.5} \Leftrightarrow [X] + {}^YAl_{0.5}$.

Contents in Al increase gradually from the less to the most evolved facies in the Pinilla pegmatite, and parallel to the decrease in the (Fe + Mn + Mg) contents (Fig. 3d). This good negative correlation is consistent with the schorl to elbaite, substitution scheme, which seems to be one of the most important substitutions in the tourmalines studied.

Although Al contents in tourmaline increase during pegmatite evolution, in the individual and less evolved facies of the Pinilla pegmatite, as well as in the pegmatitic and quartz–tourmaline veins within the leucogranite, the Al contents decrease slightly parallel to the increase in the Na contents (Fig. 3e), and therefore, follow the first substitution scheme (foitite–schorl). An opposite trend is observed for the Li-richest tourmalines (both green and pink) from the zone 3 of the pegmatite, with the enrichment in Al parallel to the decrease in Na corresponding with the third substitution scheme (elbaite–rossmanite) (Fig. 3e).

F contents in tourmaline show a similar behaviour to Na, with enrichment from the veins inside the leucogranite to the green tourmalines in the evolved zone 3, and a decrease in the pink elbaites (Figs. 3f and g). This implies that substitutional schemes include changes also in the V- and W-sites, with the exchange vector $OH_{-1}F_1$.

Discussion

In the different zones of the Pinilla rare-element pegmatite, as well as in the pegmatitic and quartz–tourmaline veins inside the associated leucogranite, tourmaline occurs as several texturally and compositionally distinct types.

Analytical data reveal that the tourmaline compositions change from Mg-rich schorl, through Al-rich schorl, to elbaite with a high rossmanite component. The occurrence of black tourmaline, compositionally intermediate tourmaline, and elbaite in the zones 1, 2 and 3 of the pegmatite respectively, suggests that the chemical variation of tourmaline has been controlled, to some degree, by the elbaite substitution $LiAlFe_{-2}$. In addition, elbaite from zone 3 has evolved toward rossmanite compositions by the $Na_{-1}Li_{-0.5}[X]Al_{0.5}$ exchange vector. Tourmaline compositions of the pegmatitic and quartz–tourmaline veins inside the leucogranite seem to have evolved via the substitutions $[X]_{-1}Al_{-1}NaFe^{2+}$ and $Mg_{-1}Fe^{2+}$. This is consistent with previous studies of the compositional evolution of tourmaline in pegmatites. For example, this sequence is similar to those described for tourmalines from the Tanco petalite-subtype pegmatite, from the border to the inner zones (Selway et al., 2000), as well as to the tourmalines from the Separation Lake petalite-subtype pegmatites (Tindle et al., 2002). It is also comparable to the crystallization sequences observed by Selway et al. (1999) for tourmalines associated with lepidolite-subtype pegmatites from the Czech Republic and from Red Cross Lake (Manitoba).

The highest Zn contents for tourmaline are observed in tourmalines with intermediate contents in Li (green schorls from zone 2). This behaviour of Zn contents has been previously described by *Tindle et al.* (2002) for tourmalines from the Pakeagama Lake area. Moreover, the Zn-richest tourmalines from Pinilla pegmatite appear in the zone with an intermediate degree of evolution, as observed by *Jolliff et al.* (1986) and by *Novák* (2000) for other pegmatitic sequences.

All the tourmalines studied have significant X-site vacancies, which indicates either the partitioning of Na into coexisting albite, or that the alkali-deficient tourmaline crystallized from a melt that was depleted in alkalis due to albite precipitation.

The stability field of tourmaline depends on different parameters, such as the activities of B and Al. In addition, temperature, $a_{\text{H}_2\text{O}}$, and contents in Fe, Mg, F, and P may be important, as they control saturation of the melt with regard to AFM phases and tourmaline (*Benard et al.*, 1985; *Holtz and Johannes*, 1991; *Gan and Hess*, 1992; *Wolf and London*, 1994, 1997). The formation of black tourmaline can remove the Fe–Mn–Mg that the pegmatite melt contains. In the Pinilla pegmatite, the occurrence of Fe–Mn phosphate nodules in zone 2, where minor tourmaline appears could be interpreted as follows: 1) the amount of B was not sufficient in bulk melt; 2) much of the B was lost prior to phosphate crystallization; 3) the presence of P decreased the stability of tourmaline by lowering the activity of Al in the melt (*Wolf and London*, 1994). The strong affinity of P with Al would favour the crystallization of phosphates instead of tourmaline (*Gan and Hess*, 1992; *Wolf and London*, 1997). The first explanation is not supported by evidence from the Pinilla pegmatite, as tourmaline crystallizes till the end of the pegmatitic differentiation in zone 3, where elbaite crystals are minor constituents. The second explanation can also be rejected, as no tourmalinization processes were observed in the country rocks (e.g. in the hornfels). Hence, it seems that the magmatic–pegmatitic system behaved as a closed or almost closed system, and no B was lost during crystallization. The third explanation thus seems to be the most plausible. Once P, Fe, Mn, and Mg have been depleted from the melt during the crystallization of the Fe–Mn phosphate nodules in zone 2, with major fractionation B and Li contents increase promoting the crystallization of Li-rich tourmaline in the apical zone 3. The Fe value increases progressively from the pegmatitic and quartz–tourmaline veins inside the leucogranite (Fe from 0.50 to 0.53), through zones 1b and 2 of the rare-element pegmatite (Fe from 0.64 to 0.98), to the evolved zone 3 (Fe = 1), reflecting the fractionation and internal evolution of the pegmatitic system. However, the decrease of the total (Fe + Mg + Mn) in the tourmalines is not so gradual, but it decreases dramatically from the point where Fe–Mn phosphates appear, i.e. from zone 2 of the pegmatite. Thus, (Fe + Mn + Mg) values change slightly from the tourmalines associated with the pegmatitic and quartz–tourmaline veins inside the leucogranite (2.36 apfu), to those tourmalines in zone 2 of the pegmatite (2.02 apfu). In contrast, for the tourmalines near the phosphate nodules in zone 2 the (Fe + Mn + Mg) values decrease to 1.62 apfu, and to 0.085 apfu for the pink elbaite in zone 3. This strong decrease in the (Fe + Mn + Mg) values for the latest tourmalines may also be related with the crystallization of the Fe–Mn phosphate masses in zone 2. These would have depleted the (Fe + Mn + Mg) contents in the melt, preferentially partitioned into the phosphate phases.

The increase in the Sn contents simultaneously with the increase in Li (Table 2) seems to be controlled by fractionation of the pegmatite-forming melt, as is also noted by *Power* (1968) for tourmalines from SW England, and by *Keller et al.* (1999) for tourmalines associated with pegmatites from the Southern Tin Belt in Central Namibia. Although high Sn contents in tourmaline (≥ 60 ppm) have been proposed as possible indicators of Sn-mineralizations (*Némec*, 1973), no Sn-enrichments have been detected related to the Pinilla pegmatite.

The chemical evolution of the tourmaline and other main phases of the pegmatite from one zone to another and some textural features in other minerals support a model of fractional crystallization for the whole pegmatite system. The lack of significant compositional variations inside the individual tourmaline crystals from the core to the rims could be explained with episodes of re-equilibration in the system during internal evolution of the pegmatite. The high Mg contents shown by the tourmalines associated with the pegmatitic and quartz–tourmaline veins within the leucogranite suggest that these veins may be derived from an earlier concentration of boron-rich fluids in the granitic chamber, prior to the generation of the Pinilla pegmatite, as it is also described by *Tindle et al.* (2002) for veins in the Pakeagma Lake Pluton (Canada).

Concluding remarks

Petrographic and microprobe data of tourmaline in the Pinilla pegmatite and associated leucogranite permit the following conclusions:

- (1) The compositional evolution of tourmaline from the pegmatitic and quartz–tourmaline veins within the leucogranite ranges from schorl–dravite to Mg-rich schorl, with a high foitite component throughout. Mg-rich schorl (with a high foitite component), and Al-rich schorl (with minor vacancies in the X-site) dominate in zones 1 and 2, inside the rare-element pegmatite. Schorl–elbaite (green crystals in hand-specimen) and elbaite with a high rossmanite component characterize tourmalines from zone 3 of the pegmatite. As expected for tourmalines of magmatic derivation, the Fe value is relatively high, ranging from 0.81 to 1.00 in the tourmalines from the pegmatite, and from 0.47 to 0.73 for the tourmalines from the pegmatitic and quartz–tourmaline veins within the leucogranite.
- (2) The most likely substitution schemes in tourmaline were $\text{Mg}_{-1}\text{Fe}_1$ and $[\text{X}]_{-1}^{\text{Y}}\text{Al}_{-1}^{\text{X}}\text{Na}_1^{\text{Y}}\text{Fe}^{2+}_1$, for the foitite–schorl series; $^{\text{Y}}\text{Fe}^{2+}_{-3} \text{ } ^{\text{Y}}\text{Al}_{1.5} \text{ } ^{\text{Y}}\text{Li}_{1.5}$, for the schorl–elbaite vector; and, $^{\text{X}}\text{Na}_{-1} \text{ } ^{\text{Y}}\text{Li}_{-0.5} [\text{X}]_1 \text{ } ^{\text{Y}}\text{Al}_{0.5}$, for the elbaite–rossmanite series. To explain the complexity of the chemical evolution in the tourmalines studied the combination of more than one exchange vector is needed, implying changes not only in the X, and Y sites, but also in the Z, V and W sites. The $(\text{OH})_{-1}\text{F}_1$ exchange vector, was operative in the tourmalines studied except in the pink elbaites from zone 3.
- (3) At intermediate levels of differentiation, in the zone 2 of the Pinilla pegmatite, Fe, Mn, and Mg preferentially fractionated into the Fe–Mn phosphate phases and, as a result, the (Fe + Mn + Mg) contents of coeval tourmaline strongly decreased.

- (4) The chemical variations observed in the tourmaline from the veins hosted by the leucogranite to the evolved zone 3, in the Pinilla pegmatite, are continuous and are consistent with a crystal fractionation model, although re-equilibration episodes during the internal evolution of the pegmatite should also be considered.

Acknowledgements

We express our gratitude to Dr. *M. Novák* and to one anonymous reviewer for their constructive comments on the manuscript. This study has been carried out with the support of the Spanish CICYT (project n° BTE 2002/01920).

References

- Benard F, Moutou P, Pichavant M* (1985) Phase relations of tourmaline leucogranites and the significance of tourmaline in silicic magmas. *J Geol* 93: 271–291
- Burns PC, MacDonald DJ, Hawthorne FC* (1994) The crystal chemistry of manganese-bearing elbaite. *Can Mineral* 32: 31–41
- Gan H, Hess PC* (1992) Phosphate speciation in potassium aluminium silicate glasses. *Am Mineral* 77: 495–506
- Gaweda A, Pieczka A, Kraczk J* (2002) Tourmalines from the Western Tatra Mountains (W-Carpathians, S-Poland): their characteristics and petrogenetic importance. *Eur J Mineral* 14: 943–955
- Hawthorne FC, Henry D* (1999) Classification of the minerals of the tourmaline group. *Eur J Mineral* 11: 201–215
- Henry DJ, Guidotti ChV* (1985) Tourmaline as a petrogenetic indicator mineral: an example from the staurolite-grade metapelites of NW Maine. *Am Mineral* 70: 1–15
- Holtz F, Johannes W* (1991) Effect of tourmaline on melt fraction and composition of first melts in quartzofeldspathic gneisses. *Eur J Mineral* 3: 527–533
- Jolliff BL, Papike JJ, Shearer CHK* (1986) Tourmaline as a recorder of pegmatite evolution: Bob Ingersoll pegmatite, Black Hills, South Dakota. *Am Mineral* 71: 472–500
- Keller P, Roda E, Pesquera A, Fontan F* (1999) Chemistry, paragenesis and significance of tourmaline in pegmatites of the Southern Tin Belt, central Namibia. *Chem Geol* 158: 203–225
- López Plaza M, Carnicero MA* (1988) El plutonismo Hercínico de la penillanura salmantino-zamorana (centro-oeste de España): Visión de conjunto en el contexto geológico regional. In: *Geología de los granitoides y rocas asociadas del macizo Hespérico*. Edit. Rueda, Madrid, pp 53–68
- Martín-Izard A, Reguilón R, Palero F* (1992) Las mineralizaciones litíferas del oeste de Salamanca y Zamora. *Estudios Geológicos* 48: 19–13
- Martínez Fernández FJ* (1974) Estudio del área metamórfica y granítica de los Arribes del Duero (Prov. de Salamanca y Zamora). Thesis, University of Salamanca, 286 p
- Morgan GBVI, London D* (1987) Alteration of amphibolitic wall-rocks around the Tanco rare-element pegmatite, Bernic Lake, Manitoba. *Am Mineral* 72: 1097–1121
- Némec D* (1973) Tin in tourmaline. *N Jb Mineral Mh* 1973: 58–63
- Novák M* (2000) Compositional pathways of tourmaline evolution during primary (magmatic) crystallization in complex (Li) pegmatites of the Moldanubicum, Czech Republic. *Mem Soc Ital Sci Nat Museo Civ Storia Nat Milano* 30: 45–56
- Power GH* (1968) Chemical variation in tourmalines from Southwest England. *Mineral Mag* 36: 1078–1098

- Roda E, Fontan F, Pesquera A, Keller P* (1998) The Fe–Mn phosphate associations from the Pinilla de Fermoselle pegmatite, Zamora, Spain: occurrence of kryzhanovskite and natrodufrénite. *Eur J Mineral* 10: 155–167
- Rodríguez-Carvajal J* (1998) FullProf: Rietveld, Profile Matching and Integrated Intensities Refinement of X-ray and/or Neutron Data (powder and/or single crystal). User's guide FullProf Software. Laboratoire Leon Brillouin (CEA-CNRS)
- Selway JB, Novák M* (1997) Experimental conditions, normalization procedures and used nomenclature for tourmaline. In: *Novák M, Selway JB* (eds) *Tourmaline 1997. Field Trip Guidebook*. Morav Museum, Brno, pp 19–21
- Selway JB, Novák M, Hawthorne F, Cerny P, Ottolini L, Kyser TK* (1998) Rossmanite, $[X](LiAl_2)Al_6(Si_6O_{18})(BO_3)_3(OH)_4$, a new alkali-deficient tourmaline: description and crystal structure. *Am Mineral* 83: 896–900
- Selway JB, Novák M, Cerny P, Hawthorne FC* (1999) Compositional evolution of tourmaline in lepidolite-subtype pegmatites. *Eur J Mineral* 11: 569–584
- Selway JB, Cerny P, Hawthorne FC, Novák M* (2000) The Tanco pegmatite at Bernic Lake, Manitoba. XIV. Internal tourmaline. *Can Mineral* 38: 877–891
- Tindle AG, Breaks FW, Selway JB* (2002) Tourmaline in petalite-subtype granitic pegmatites: evidence of fractionation and contamination from the Pakeagama Lake and Separation Lake areas of Northwestern Ontario, Canada. *Can Mineral* 40–3: 753–788
- Wolf MB, London D* (1994) Apatite dissolution into peraluminous haplogranitic melts: an experimental study of solubilities and mechanisms. *Geochim Cosmochim Acta* 58: 4127–4145
- Wolf MB, London D* (1997) Boron in granitic magmas: stability of tourmaline in equilibrium with biotite and cordierite. *Contrib Mineral Petrol* 130: 12–30

Authors' addresses: *E. Roda* (corresponding author; e-mail: npproroe@lg.ehu.es), *A. Pesquera* (e-mail: npppepea@lg.ehu.es), and *P. P. Gil* (e-mail: nppgicrp@lg.ehu.es), Departamento de Mineralogía y Petrología, Facultad de Ciencia y Tecnología, Universidad País Vasco/EHU, Apdo. 644, E-48080 Bilbao, Spain; *J. Torres-Ruiz* (e-mail: jotorres@ugr.es), Departamento de Mineralogía y Petrología, Facultad de Ciencias, Universidad Granada, Fuentenueva s/n, E-18002 Granada, Spain; *F. Fontan*, Laboratoire Cristallographie et Minéralogie, URA-067-Université Paul Sabatier de Toulouse, Allées Jules-Guesde 39, F-31400 Toulouse, France